

# OSNR monitoring for QPSK and 16-QAM systems in presence of fiber nonlinearities for digital coherent receivers

Zhenhua Dong,<sup>1,\*</sup> Alan Pak Tao Lau,<sup>1</sup> and Chao Lu<sup>2</sup>

<sup>1</sup>Photonics Research Centre, Department of Electrical Engineering, The Hong Kong Polytechnic University, Hung Hom, Kowloon, Hong Kong, China

<sup>2</sup>Photonics Research Centre, Department of Electronic and Information Engineering, The Hong Kong Polytechnic University, Hung Hom, Kowloon, Hong Kong, China

\*dong.keke@gmail.com

**Abstract:** OSNR monitoring is indispensable for coherent systems to ensure robust, reliable network operation and potentially enable impairment-aware routing for future dynamic optical networks. In a long-haul transmission link with chromatic dispersion (CD) and fiber nonlinearity, it is difficult to distinguish between amplifier noise and fiber nonlinearity induced distortions from received signal distributions even after various transmission impairment compensation techniques, thus resulting in grossly inaccurate OSNR estimates. Based on the received signal distributions after carrier phase estimation (CPE), we propose to characterize the nonlinearity-induced amplitude noise correlation across neighboring symbols and incorporate such information into error vector magnitude (EVM) calculation to realize fiber nonlinearity-insensitive OSNR monitoring. For a transmission link up to 1600 km and signal launched power up to 2 dBm, experimental results for 112 Gb/s polarization-multiplexed quadrature phase-shift keying (PM-QPSK) demonstrate an OSNR monitoring range of 10-24 dB with a maximum estimation error below 1 dB. For 224 Gb/s PM-16-quadrature amplitude modulation (PM-16-QAM) systems, simulation results demonstrate an OSNR monitoring range of 18-28 dB with a maximum estimation error below 1 dB. Tolerance of the proposed OSNR monitoring technique to different pulse shapes, timing phase offsets, polarization dependent loss (PDL), polarization-mode dispersion (PMD) and WDM effects are also investigated through simulations.

©2012 Optical Society of America

**OCIS codes:** (060.1660) Coherent communications; (060.2330) Fiber optics communications; (060.4261) Networks, protection and restoration; (060.4370) Nonlinear optics, fibers.

---

## References and links

1. D. C. Kilper, S. Chandrasekhar, L. Buhl, A. Agarwal, and D. Maywar, "Spectral monitoring of OSNR in high speed networks," in European Conference and Exhibition on Optical Communication (ECOC), 2002, paper 7.4.4.
2. J. H. Lee, D. K. Jung, C. H. Kim, and Y. C. Chung, "OSNR monitoring technique using polarization nulling method," *IEEE Photon. Technol. Lett.* **13**(1), 88-90 (2001).
3. S. D. Dods and T. B. Anderson, "Optical performance monitoring technique using delay tap asynchronous waveform sampling," in Proc. OFC'06, Anaheim, California, Mar. 2006, Paper OThP5.
4. J. A. Jargon, X. Wu, and A. E. Willner, "Optical performance monitoring using artificial neural networks trained with eye-diagram parameters," *IEEE Photon. Technol. Lett.* **21**(1), 54-56 (2009).
5. E. Ip, A. P. T. Lau, D. J. F. Barros, and J. M. Kahn, "Coherent detection in optical fiber systems," *Opt. Express* **16**(2), 753-791 (2008).
6. S. J. Savory, "Digital coherent optical receivers: Algorithms and subsystems," *IEEE J. Sel. Top. Quantum Electron.* **16**(5), 1164-1179 (2010).

7. S. L. Woodward, L. E. Nelson, M. D. Feuer, X. Zhou, P. D. Magill, S. Foo, D. Hanson, H. Sun, M. Moyer, and M. O'Sullivan, "Characterization of real-time PMD and chromatic dispersion monitoring in a high-PMD 46-Gb/s transmission system," *IEEE Photon. Technol. Lett.* **20**(24), 2048–2050 (2008).
8. F. N. Hauske, M. Kuschnerov, B. Spinnler, and B. Lankl, "Optical performance monitoring in digital coherent receivers," *J. Lightwave Technol.* **27**(16), 3623–3631 (2009).
9. F. Pittalà, F. N. Hauske, Y. Ye, N. G. Gonzalez, and I. T. Monroy, "Joint PDL and in-band OSNR monitoring supported by data-aided channel estimation," in *Proc. OFC'12, Los Angeles, Mar. 2012*, Paper OW4G.
10. D. J. Ives, B. C. Thomsen, R. Maher, and S. Savory, "Estimating OSNR of equalised QPSK signals," in *Proc. European Conference and Exhibition on Optical Communication (ECOC), 2011*, Paper Tu.6.A.6.
11. R. Schmogrow, B. Nebendahl, M. Winter, A. Josten, D. Hillerkuss, S. Koenig, J. Meyer, M. Dreschmann, M. Huebner, C. Koos, J. Becker, W. Freude, and J. Leuthold, "Error vector magnitude as a performance measure for advanced modulation formats," *IEEE Photon. Technol. Lett.* **24**(1), 61–63 (2012).
12. M. Mayrock and H. Haunstein, "Optical monitoring for non-linearity identification in CO-OFDM transmission systems," in *Proc. OFC'08, San Diego, CA, Feb. 2008*, Paper JThA58.
13. E. Ip, "Nonlinear compensation using backpropagation for polarization-multiplexed transmission," *J. Lightwave Technol.* **28**(6), 939–951 (2010).
14. Z. H. Dong, A. P. T. Lau, and C. Lu, "OSNR monitoring for PM-QPSK systems in presence of fiber nonlinearities for digital coherent receivers," in *Proc. Optoelectronic Communication Conference (OECC), 2012*, Paper 6B3–3.
15. J. Renaudier, G. Charlet, O. Bertran-Pardo, H. Mardoyan, P. Tran, M. Salsi, and S. Bigo, "Transmission of 100 Gb/s Coherent PDM-QPSK over 16 x 100 km of Standard Fiber with erbium amplifiers," *Opt. Express* **17**(7), 5112–5119 (2009).
16. A. H. Gnauck, P. J. Winzer, S. Chandrasekhar, X. Liu, B. Zhu, and D. W. Peckham, "Spectrally efficient long-haul WDM transmission using 224-Gb/s polarization-multiplexed 16-QAM," *J. Lightwave Technol.* **29**(4), 373–377 (2011).
17. P. Poggiolini, A. Carena, V. Curri, G. Bosco, and F. Forghieri, "Analytical modeling of nonlinear propagation in uncompensated optical transmission links," *IEEE Photon. Technol. Lett.* **23**(11), 742–744 (2011).
18. F. Vacondio, O. Rival, C. Simonneau, E. Grellier, A. Bononi, L. Lorcy, J. C. Antona, and S. Bigo, "On nonlinear distortions of highly dispersive optical coherent systems," *Opt. Express* **20**(2), 1022–1032 (2012).
19. A. Bononi, P. Serena, N. Rossi, and D. Sperti, "Which is the dominant nonlinearity in long-haul PDM-QPSK coherent transmissions?" in *European Conference and Exhibition on Optical Communication (ECOC), 2010*, Th.10.E.1.
20. A. Bononi, N. Rossi, and P. Serena, "Transmission limitations due to fiber nonlinearity," in *Proc. OFC'11, Los Angeles, Mar. 2011*, Paper OW07.
21. A. P. T. Lau, S. Rabbani, and J. M. Kahn, "On the statistics of intra-channel four-wave mixing in phase-modulated optical communication systems," *J. Lightwave Technol.* **26**(14), 2128–2135 (2008).
22. Optical Monitoring for DWDM Systems. ITU-T recommendation G.697, June 2004.
23. VPIsystems™, "VPItransmissionMaker™".
24. X. Zhou, J. Yu, and P. D. Magill, "Cascaded two-modulus algorithm for blind polarization de-multiplexing of 114-Gb/s PDM-8-QAM optical signals," in *Proc. OFC'09, San Diego, Mar. 2009*, Paper OWG3.
25. Y. L. Gao, A. P. T. Lau, S. Y. Yan, and C. Lu, "Low-complexity and phase noise tolerant carrier phase estimation for dual-polarization 16-QAM systems," *Opt. Express* **19**(22), 21717–21729 (2011).
26. O. Vassilieva, T. Hoshida, X. Wang, J. Rasmussen, H. Miyata, and T. Naito, "Impact of polarization dependent loss and cross-phase modulation on polarization multiplexed DQPSK signals," in *Proc. OFC'08, San Diego, CA, Feb. 2008*, Paper OThU6.

---

## 1. Introduction

Optical-signal-to-noise ratio (OSNR) is one of the most critical parameters to assess the quality of transmission link and system performance that facilitate link fault localization with fast protection path switching. In reconfigurable and future dynamic optical networks, flexible payload switching, wavelength allocation and potentially impairment-aware routing would not be possible without the information of link OSNR. Techniques based on optical spectral analysis [1], polarization nulling [2], asynchronous histograms [3] and neural networks [4] among others have been proposed for OSNR monitoring. However, some of these methods are only applicable to certain modulation format/pulse shapes and are not applicable to polarization-multiplexed (PM) systems. In addition, they may not work in realistic communication systems where other deterministic and statistical channel impairments are present.

Advanced coherent modulation formats such as PM-QPSK and PM-16-QAM with digital coherent receivers and appropriate transmission impairment compensation algorithms have emerged as the most promising solution for the next generation high capacity optical

transmission networks operating at 100-Gbps and beyond [5, 6]. It also enables a promising and comprehensive built-in optical performance monitoring (OPM) at the receiver for free. Chromatic dispersion (CD), polarization-mode dispersion (PMD) and polarization-dependent loss (PDL) can be estimated through analyzing the filter impulse response which is an indicator of the inverse impulse response of the channel [7, 8]. Meanwhile, although OSNR monitoring is not as easy as reading off filter taps, ASE-noise-induced distortions can be separated from all the other linear transmission impairments in a digital coherent receiver and reliable OSNR can still be estimated with further processing of the received signals. Pittalà proposed an OSNR monitoring technique [9] through data-aided FD channel estimation employing very short training sequences. Other methods are derived from wireless communications including the estimation of OSNR through the moments of the radial distribution of equalized PM-QPSK signals in digital coherent receivers [10] or using error vector magnitude (EVM) for non data-aided receivers [11]. However, most of the currently deployed long-haul optical communication systems operate in the weakly nonlinear regime which is a tradeoff between mitigating the effect of ASE noise and fiber nonlinearities. The OSNR increases with the signal launched power but so does the impact of fiber nonlinearities. Nonlinear distortions are typically treated as noise and are indistinguishable from amplifier noise by the standard DSP platform [6, 12] since fiber nonlinearity compensation algorithms such as digital back-propagation [13] is too complex to be realized at present. Therefore, current OSNR estimation techniques using digital coherent receivers will considerably underestimate the OSNR for long-haul transmission systems and a fiber-nonlinearity-insensitive OSNR monitoring technique is yet to be developed to realize accurate OSNR monitoring in long-haul optical communication systems.

In this paper, we extend our preliminary investigation [14] and propose to use the received signals after carrier phase estimation (CPE) in a standard digital coherent receiver and characterize the fiber nonlinearity induced amplitude noise correlation among neighboring symbols as a quantitative measure of nonlinear distortions to the signal. This nonlinear measure is shown to only depend on signal launched power but not OSNR and hence fiber nonlinear distortions can be isolated from ASE noise. In this case, nonlinearity-insensitive OSNR monitoring can be achieved by incorporating/calibrating such amplitude noise correlations into an EVM-based OSNR estimator. Experimental as well as simulation results demonstrate an OSNR monitoring range of 10-24 dB with a maximum estimation error of 1.0 dB for 112 Gb/s PM-QPSK systems and 18-28 dB with a maximum estimation error of 1.0 dB for 224 Gb/s PM-16-QAM systems. The maximum signal launched power is 4 dBm for transmission distance up to 800 km and 2 dBm for longer distance up to 1600 km. It should be noted that signal launched power above 2 dBm at such transmission distances are already considerably higher than the optimal signal power level for realistic 28G baud PM-QPSK and PM-16-QAM systems [15, 16] and hence the proposed technique is applicable to systems with strong fiber nonlinearity. In addition, the proposed OSNR monitoring technique is shown to be tolerant towards the effects of timing phase offsets, different signal pulse shapes, PDL and first-order PMD. Furthermore, simulations for WDM systems show that while inter-channel nonlinearities such as cross-phase modulation (XPM) can introduce further distortions to the signal, appropriate calibrations to the proposed OSNR estimator can be performed to maintain the OSNR monitoring accuracy.

## 2. Theoretical foundations

### 2.1 OSNR estimation based on received signal distributions and error vector magnitude (EVM)

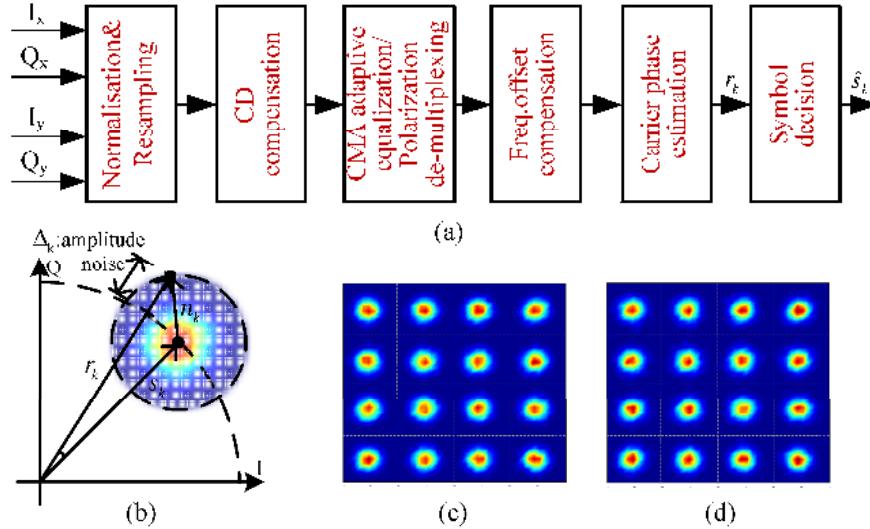


Fig. 1. (a) Standard signal processing blocks in a digital coherent receiver; (b) Graphical illustration of received signal and amplitude noise  $\Delta_k$ ; Received 16-QAM distributions with (c) -4 dBm signal launched power and 18 dB OSNR (d) 4 dBm signal launched power and 26 dB OSNR over a 800-km link. As evident from the figures, amplifier noise and fiber nonlinearity effects will induce similar distortions to the received signal distribution and therefore it is not easy to distinguish between them for accurate OSNR monitoring.

Consider a coherent optical transmission system with a polarization-multiplexed  $M$ -QAM signal transmitted over a multi-span link with inline optical amplifiers to compensate for signal loss incurred throughout the span. Transmission impairments such as CD, PMD, fiber nonlinearity and amplified spontaneous emission (ASE) noise generated from inline amplifiers will distort the received signal and possibly limit system performance. Neglecting electrical noise generated from receiver circuitries, fiber nonlinearity and multi-channel effects, the received signal in a digital coherent receiver is sampled and processed in a digital signal processing unit (DSP) with standard signal processing algorithms such as normalization, re-sampling, CD/PMD compensation, laser frequency offset and carrier phase estimation (CPE) as shown in Fig. 1(a). In this case, the  $k^{\text{th}}$  received symbol of the CPE output in one particular polarization can be represented as

$$r_k = s_k + n_k \quad (1)$$

where  $s_k$  is the transmitted  $M$ -QAM symbol and  $n_k$  models the collective ASE noise generated by inline optical amplifiers which is a band-limited complex circularly symmetric zero-mean Gaussian random process with covariance matrix  $\sigma^2 I$ . Many techniques exist to estimate OSNR from  $r_k$ . In particular, we use the principle of EVM in [11] and propose an OSNR estimate through

$$OSNR_{Estimated} = \frac{P_{in}}{P_{ASE}} = \frac{\mathbf{E}(|\hat{s}_k|^2)}{\mathbf{E}(|n_k|^2)} \quad (2)$$

where  $P_{in}$  is the signal power,  $P_{ASE}$  accounts for the ASE noise power and  $\hat{s}_k$  is the symbol after decision as shown in Fig. 1(a) and  $\mathbf{E}(\cdot)$  denotes expectation.

However, in realistic long-haul transmission systems where fiber nonlinearity impairs system performance, the interaction of nonlinearity, CD and ASE noise results in additional distortions that cannot be easily mitigated by standard DSP techniques. Recently, a zero-mean complex circularly symmetric additive Gaussian model for such nonlinear distortions has been analytically proposed and experimentally validated [17, 18] for long-haul coherent transmission links without in-line dispersion compensation. At a high baud rate, i.e. 28G baud/s, optical pulses are largely overlapped due to CD and it can be shown that intra-channel nonlinearities such as intra-channel four-wave mixing (IFWM) dominate over inter-channel nonlinearities such as cross-phase modulation (XPM) [19, 20]. Considering the effect of intra-channel nonlinearity only, Eq. (1) can be re-written as

$$r_k = s_k + n'_k = s_k + n_k + v_k \quad (3)$$

where  $n'_k = n_k + v_k$  consists of ASE noise  $n_k$  and nonlinearity-induced distortions  $v_k$ . With the EVM methodology,  $v_k$  become addition distortions that can significantly affect the OSNR estimate from the received signal distributions. Figure 1(c) and 1(d) shows the received signal distributions obtained from simulations for a 224 Gb/s PM-16-QAM signal transmitted over 800 km of standard single-mode fibers (SSMF) where the signal launched power (OSNR) are  $-4$  dBm (18 dB) and 4 dBm (26 dB) respectively. It is clear from the figures that despite the difference in OSNR, fiber nonlinearity effects result in additional distortions and can become indistinguishable from ASE noise. Thus if we naively use the EVM method by simply measuring the ‘size’ of the ‘clouds’ in the received signal distributions, the OSNR estimates are given by

$$OSNR_{Estimated} = \frac{\mathbf{E}(|\hat{s}_k|^2)}{\mathbf{E}(|n'_k|^2)} = \frac{\mathbf{E}(|\hat{s}_k|^2)}{\underbrace{\mathbf{E}(|n_k|^2) + \mathbf{E}(|v_k|^2) + \mathbf{E}(n_k v_k^*) + \mathbf{E}(n_k^* v_k)}_{P_{NL}}} = \frac{P_{in}}{P_{ASE} + P_{NL}} \quad (4)$$

which can significantly under-estimate the true OSNR. Consequently, techniques to isolate fiber nonlinearity effects from ASE noise are to be developed in order to realize accurate OSNR monitoring in coherent links in presence of fiber nonlinearity.

## 2.2 Calibrating nonlinearity induced-amplitude noise correlations across received symbols into EVM-based OSNR estimates

The interaction of fiber nonlinearity, CD and ASE noise will produce distortions such as IFWM that are shown to be correlated across neighboring symbols even after appropriate linear impairment compensation [21]. In particular, the phase as well as amplitude noise across neighboring symbols are shown to be correlated. Denoting  $\Delta_k$  as the amplitude noise of the  $k^{\text{th}}$  received symbol, let the autocorrelation function (ACF) of amplitude noise across neighboring symbols be

$$R_{\Delta}(m) = \mathbf{E}[\Delta_k \Delta_{k+m}]. \quad (5)$$

Figure 2 compares  $|R_{\Delta}(m)|$  of a 112 Gb/s PM-QPSK system and a 224 Gb/s PM-16-QAM system obtained from simulations for various signal launched powers and OSNR values. The transmission distance is 800 km without inline optical CD compensation and the received signals are sampled and processed by standard signal processing blocks depicted in Fig. 1(a) and the amplitude noise autocorrelation are calculated accordingly from the received signal distribution after carrier phase estimation. From the figure, it is clear from  $|R_{\Delta}(m)|$  that the

amplitude noise is correlated across neighboring symbols. Also, as  $|R_{\Delta}(0)|$  is basically the amplitude noise variance in each received symbol, it would vary with both signal launched power and OSNR as reflected in the figure. However,  $|R_{\Delta}(1)|, |R_{\Delta}(2)|, |R_{\Delta}(3)| \dots$  seem to only depend on signal launched power and is quite insensitive to OSNR. This can be explained as follows: with appropriate optical and electrical filtering in a transmission link, ASE noise  $n_k$  of the received symbols  $r_k$  should be uncorrelated across neighboring symbols. However, CD induces pulse overlapping during transmission and the pulses interact with each other through fiber nonlinearity and consequently result in additional nonlinear distortions  $v_k$  in  $r_k$ . As  $v_k$  originates from neighboring symbols, it is intuitive to expect that  $v_k$  is correlated across neighboring symbols and such correlations are largely attributed to nonlinear interactions between signal pulses rather than signal-ASE noise or ASE noise-ASE noise interactions.

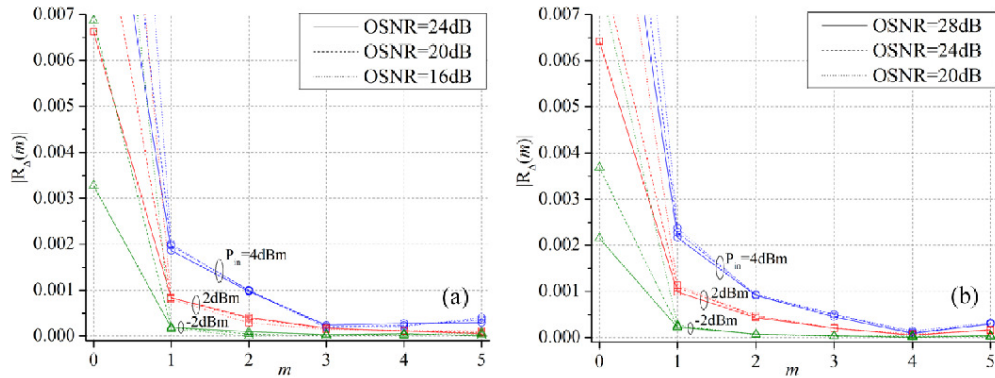


Fig. 2. Autocorrelation of fiber-nonlinearity induced amplitude noise  $|R_{\Delta}(m)|$  for a (a) 112 Gb/s PM-QPSK system and (b) 224 Gb/s PM-16-QAM system with various signal launched powers and OSNR values. The transmission distance is 800 km without inline optical CD compensation and the received signals are sampled and processed by standard DSP blocks depicted in Fig. 1(a) and the amplitude noise autocorrelation are calculated accordingly from the received signal distribution after carrier phase estimation. From the figure,  $R_{\Delta}(1)$  only depends on signal launched power and is insensitive to ASE noise and hence can be used to isolate fiber nonlinearity effects from ASE noise.

With such observation and insight, one can leverage the unique properties of  $|R_{\Delta}(m)|$  to isolate nonlinear distortions from ASE noise and realize fiber-nonlinearity-insensitive OSNR monitoring. In particular, one can use  $|R_{\Delta}(1)|$  multiplied by a calibration factor  $\xi$  as a measure/estimate of the amount of nonlinear distortions  $P_{NL}$  in the received signal  $r_k$ . The calibration factor  $\xi$  only depends on the transmission distance  $L$  and is optimized over different signal launched powers and OSNR values by the following calibration process: 1) Obtain received signal data set (through simulations or experiments) for various launched powers and OSNR values; 2) Calculate OSNR through Eq. (6) as a function of  $\xi$  for each launched power and OSNR value; 3) Optimize  $\xi$  so that the maximum monitoring error for the whole data set is minimized. 4) Store the optimized  $\xi$  (as a function of distance) in a look-up table which will be used in the actual monitoring process. We simulated an 800-km CD-uncompensated link with standard receiver DSP blocks shown in Fig. 1(a). The ACF  $|R_{\Delta}(m)|$  is calculated from  $r_k$  and  $\hat{s}_k$  accordingly and Fig. 3 compares  $|R_{\Delta}(1)| \times \xi$  with  $P_{NL}$  for various signal launched powers and OSNR values. With an optimally chosen  $\xi$ , we can

see that the  $|R_{\Delta}(1)| \times \xi$  closely estimate  $P_{NL}$  and are quite insensitive to different OSNR values. Similar results are obtained for PM-16-QAM systems but will be omitted here.

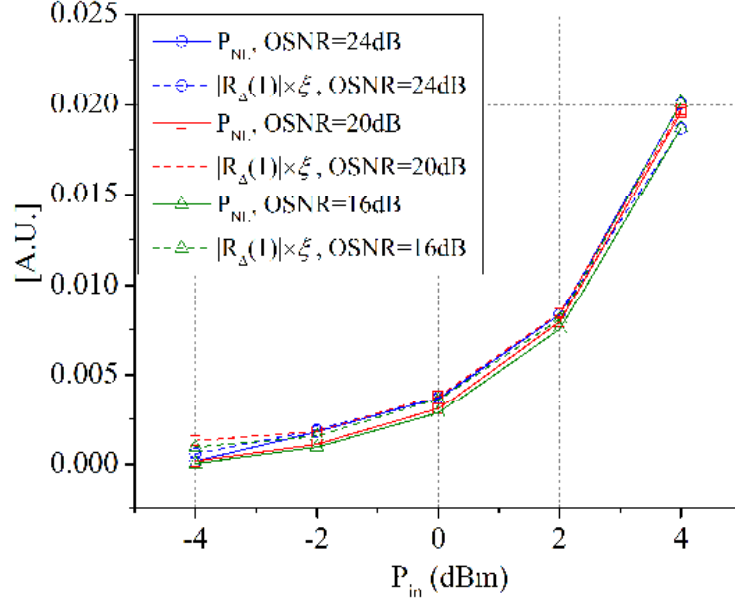


Fig. 3.  $|R_{\Delta}(1)| \times \xi$  and nonlinear noise power  $P_{NL}$  as a function of signal launched power in a 800-km CD uncompensated link. The optimal  $\xi$  is calibrated to be 10.2.

The term  $|R_{\Delta}(1)| \times \xi$  is incorporated in the OSNR estimator in Eq. (2) and thus a nonlinearity-insensitive OSNR estimation can be obtained by

$$OSNR_{Estimated} = \frac{\mathbf{E}(|\hat{s}_k|^2)}{\mathbf{E}(|n'_k|^2) - |R_{\Delta}(1)| \times \xi}. \quad (6)$$

It should be noted that the received signals in both polarization multiplexed tributaries are used for the OSNR estimation in Eq. (6). Moreover, phase noise correlation can also be used to calibrate and estimate  $P_{NL}$  and serve the same purpose of realizing accurate OSNR monitoring in presence of fiber nonlinearity. We choose to use amplitude noise correlation instead because of its robustness against additional phase noise effects such as laser frequency offsets and laser phase noise and corresponding DSP techniques to mitigate them might not be perfect in practice.

### 3. Experimental and simulation results for 112 Gb/s PM-QPSK and 224 Gb/s PM-16-QAM systems

#### 3.1 Experimental Results for 112 Gb/s PM-QPSK systems

Experiments have been performed to demonstrate the validity of the proposed OSNR monitoring technique for 112 Gb/s PM-QPSK systems. The experimental configuration is shown in Fig. 4. At the transmitter side, an external cavity laser (ECL) laser at 1550.12nm is modulated with an I/Q modulator driven by 28G baud pseudo random bit sequences (PRBS) of length  $2^{31}-1$  to produce Non-Return-to-Zero (NRZ) QPSK signals. Polarization division multiplexing is achieved by splitting the signal through a polarization beam splitter (PBS) into two branches, delaying one branch, and recombining the signal through a polarization beam

combiner (PBC). The signal is then amplified and launched into the fiber recirculating loop with a transmitted power ranging from  $-4$  to  $4$  dBm to realize various levels of fiber nonlinearity. The loop consists of a span of 80 km SSMF, erbium-doped fiber amplifier (EDFA), an attenuator placed before the EDFA to realize various OSNR values from 10 to 24 dB and also a 5nm optical band-pass filter (BPF) for channel power equalization. At the loop output, ten percent of the light is tapped into an optical spectrum analyzer (OSA) to obtain the reference (true) OSNR using out-of-band noise measurement [22]. Here and throughout the paper, the OSNR will be referred to the 0.4 nm bandwidth which corresponds to the whole signal bandwidth. The rest of the signal is filtered by a 3th order Gaussian optical BPF having 0.4 nm bandwidth and enters an integrated coherent receiver. The linewidth of transmitter and local oscillator (LO) are 150 kHz and 100 kHz respectively and the frequency offset is set to be 1 GHz. The coherently detected signal are sampled by a 50 G samples/s real-time oscilloscope and then processed offline with the following DSP algorithms: 1) Normalization and resampling to 2 samples/symbol; 2) Chromatic dispersion compensation using a finite impulse response filter [6]; 3) Adaptive equalization/PMD compensation/polarization demultiplexing with constant modulus algorithm (CMA) [6]; 4) Frequency offset compensation and carrier phase estimation [6]; 5) Symbol decision, amplitude noise correlation calculation through (5) and OSNR estimate through (6). In our experiments, 100000 symbols are used for the OSNR estimation which only requires an acquisition time of a few microseconds.

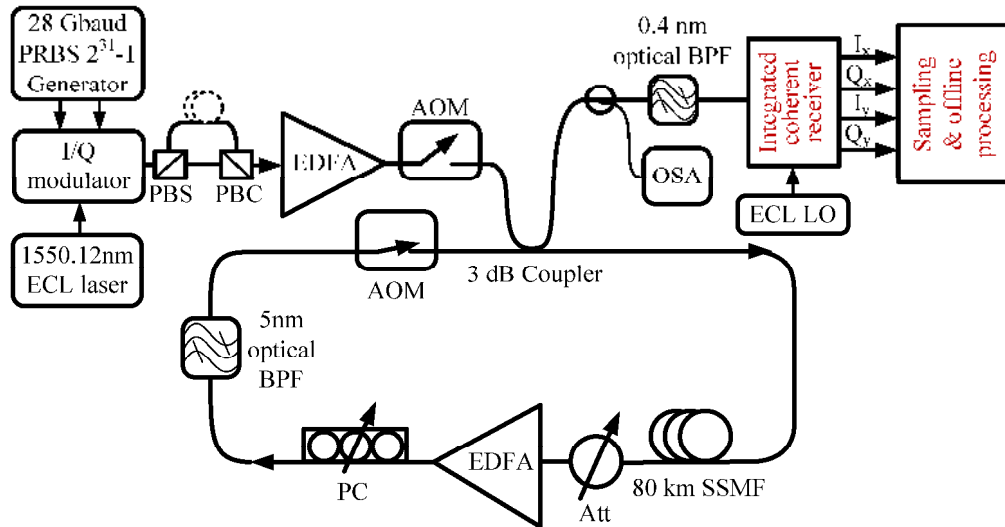


Fig. 4. System configuration for a 112Gbit/s PM-QPSK system without inline dispersion compensation. Att: attenuator, AOM: acousto-optic modulator, BPF: band-pass filter, ECL: external cavity laser, EDFA: erbium-doped fiber amplifier, PBS: polarization beam splitter, PBC: polarizing beam combiner, PC: polarization controller, OSA: optical spectrum analyzer, SSMF: standard single-mode fiber.

It is well known that practical systems suffer from impairments such as imperfect matching filters and transceiver imperfections which introduce additional distortions to the received signal. We first conducted a back-to-back experiment to estimate and ‘calibrate out’ such imperfections [10, 18].

With the received symbols obtained from experiments, the autocorrelation of fiber nonlinearity-induced amplitude noise are shown in Fig. 5 and the OSNR estimates before and after calibration with  $|R_{\lambda}(1)| \times \xi$  are shown for comparisons in Fig. 6. For each transmission distance, the calibration factor  $\xi$  is obtained from a look-up table described in the previous



section. When  $|R_{\Delta}(1)| \times \xi$  is not incorporated, the OSNR is significantly under-estimated as the nonlinear distortions are treated as ASE noise in the OSNR estimates and the estimation error generally increases with input power due to enhanced nonlinearity effects. With the calibration based on  $|R_{\Delta}(1)| \times \xi$ , the OSNR estimation error is largely reduced and the maximum errors are 0.82 dB, 0.93 dB, 0.77 dB and 1.0 dB for 400 km, 800 km, 1200 km and 1600 km transmissions respectively. The dependence of the optimized  $\xi$  on transmission distance is shown in Fig. 7 where it generally increases with distance. This is to be expected as nonlinear effects are known to build up with transmission distance [18]. It should be noted that signal launched power above 2 dBm are considerably higher than the optimal signal power level for realistic 28G baud PM-QPSK and PM-16-QAM systems [15, 16], thus illustrating the proposed technique will still function well in highly nonlinear systems.

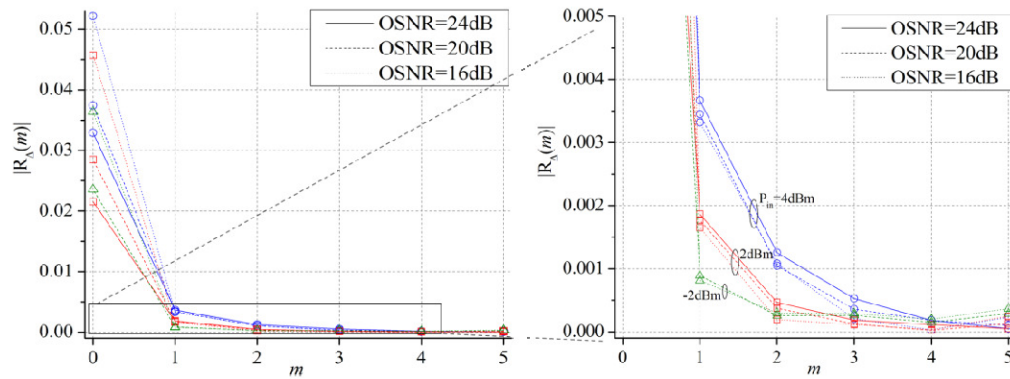


Fig. 5. Autocorrelation of fiber nonlinearity-induced amplitude noise experimentally obtained from a 112 Gb/s PM-QPSK system in a 800-km CD uncompensated link with standard DSP algorithms for transmission impairment compensation for various signal launched powers and OSNR values.

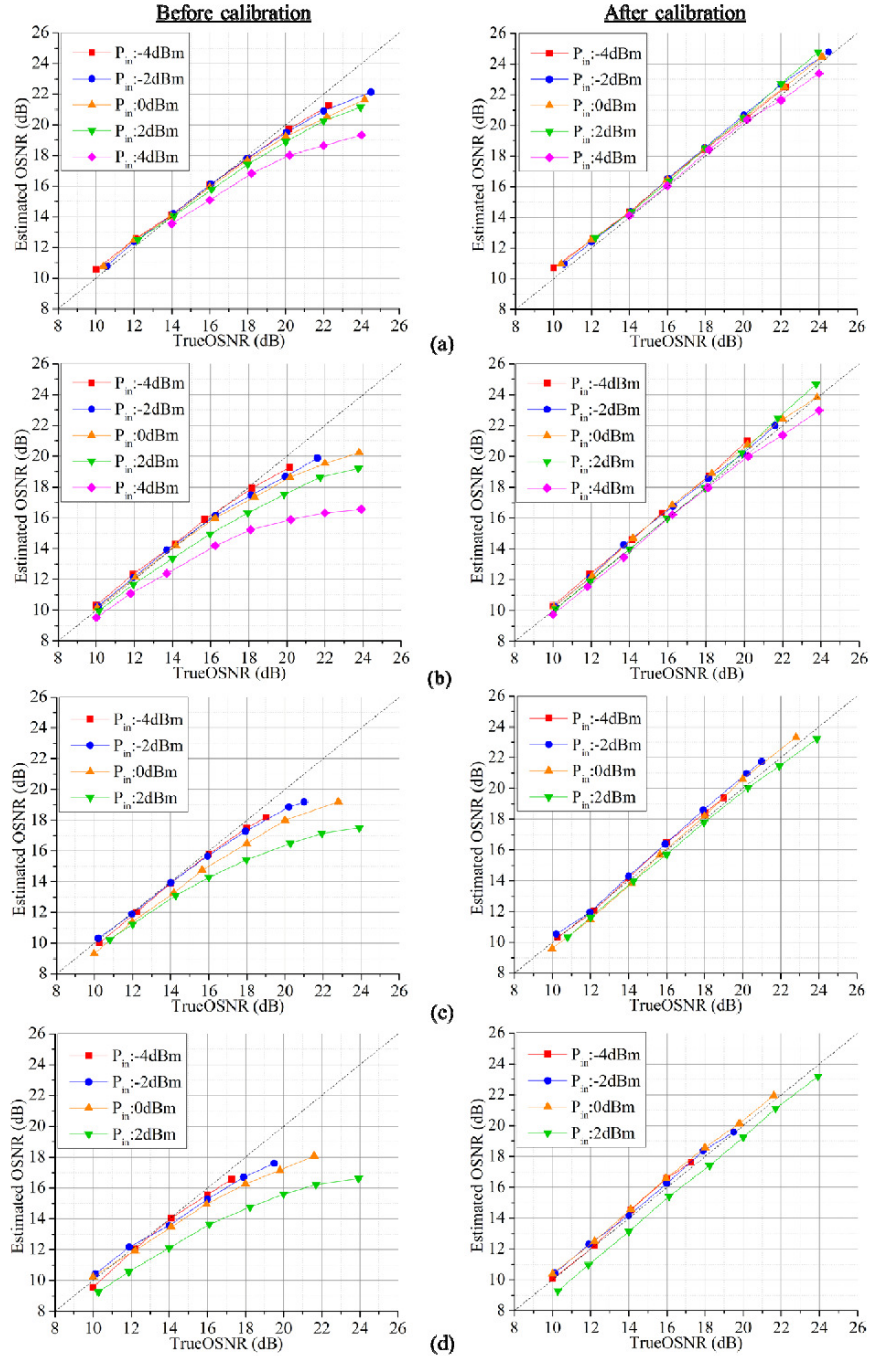


Fig. 6. Estimated OSNR vs true OSNR experimentally obtained from a 112 Gb/s PM-QPSK system for various signal launched powers and OSNR values (a) after 400 km transmission and calibrated with  $\zeta = 9$ . The maximum estimation error is 0.82 dB; (b) after 800 km transmission and calibrated with  $\zeta = 10.5$ . The maximum estimation error is 0.93 dB; (c) after 1200 km transmission and calibrated with  $\zeta = 11.5$ . The maximum estimation error is 0.77 dB; (d) after 1600 km transmission and calibrated with  $\zeta = 12.5$ . The maximum estimation error is 1.0 dB.

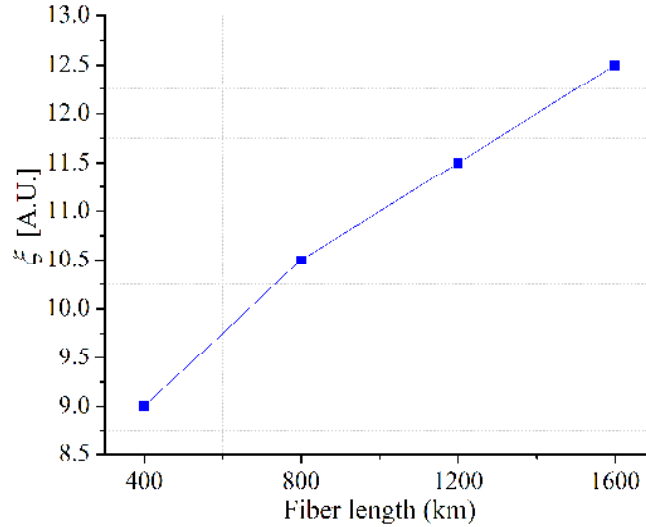


Fig. 7. The optimized calibration factor  $\xi$  vs. transmission distance for a 112 Gb/s PM-QPSK system for realizing nonlinearity-insensitive OSNR monitoring.

### 3.2 Simulation results for 224 Gb/s PM-16-QAM systems

For 224 Gb/s PM-16-QAM systems, simulations using VPI [23] are performed to demonstrate the validity of the proposed OSNR monitoring technique. In the simulation setup, the 16-QAM signals are generated by a four-level-driven I/Q modulator at the transmitter side. In the receiver DSP, the Cascaded Multi-Modulus Algorithm (CMMA) [24] is added after the standard Constant Modulus Algorithm (CMA) to better equalize the 16-QAM signals and the CPE algorithm reported in [25] is used. The rest of system setup is similar to that shown in Fig. 4.

In order to investigate the robustness of the proposed OSNR monitoring technique against different signal pulse shapes, timing phase offsets, PDL and first-order PMD effects, we studied the performance of our proposed OSNR monitor in NRZ-PM-16-QAM and 50% Return-to-Zero (RZ)-PM-16-QAM systems and a fiber link with PDL ranging from 0 to 4 dB (with 0° and 45° angles between signal state of polarization (SOP) and PDL axis) using the distributed PDL model described in [26] and differential group delay (DGD) values ranging from 0 to 20 ps (with 0°, 22.5° and 45° angles between signal SOP and fiber principle states of polarization (PSP)). The timing phases considered include 0, 1/8, 1/4 and 3/8 symbols away from optimal sampling instants at the pulse peaks.

More than a hundred OSNR monitoring curves corresponding to various pulse shapes, timing phase offsets, PDL and PMD values are generated by simulations. For each transmission distance, the calibration factor  $\xi$  has been optimized over different launched powers, OSNRs, pulse shapes, PDL and PMD effects for optimal OSNR estimation performance. Typical OSNR estimation results before and after calibration are shown in Fig. 8. For an OSNR monitoring range from 18 to 28 dB, the maximum monitoring errors are 0.35 dB, 0.94 dB, 0.53 dB and 1.0 dB for 400 km, 800 km, 1200 km and 1600 km transmissions respectively when PDL and PMD effects are absent. The maximum monitoring errors become 0.5 dB, 1.1 dB, 0.82 dB and 1.18 dB respectively when PDL is present. PMD further increases the maximum monitoring errors to 0.9 dB, 1.73 dB, 1.81 dB and 1.98 dB for 400 km, 800 km, 1200 km and 1600 km transmissions respectively. The increased estimation errors are partly due to the OSNR monitoring range shifting to higher values where the ASE noise is relatively small and thus the monitoring performance is more vulnerable to the other

distortions such as PMD. However, the estimation errors still remain on a reasonably low level and illustrates that our technique is applicable to different pulse shapes and rather insensitive to PDL and PMD effects. We would like to note that the effect of PMD on our proposed OSNR monitoring technique can potentially be further reduced by first determining the angle between SOP and PSP and the DGD value from the CMA/CMMA taps and calibrate a factor  $\xi$  specific to different angles and DGD values.

The optimized calibration factor  $\xi$  versus transmission distance is shown in Fig. 9. It should be noted that  $\xi$  is not transmission distance independent as shown in Fig. 7 and 9 and thus in some cases, i.e. in reconfigurable optical systems where the transmission distance varies, inaccurate estimation of transmission distance may affect the OSNR measurement accuracy. For future reconfigurable digital coherent systems without inline dispersion compensation, the transmission distance may be obtained from network management systems from upper layer protocols. In case this is not available, one can look at the accumulated CD that can be read out from the filter taps of the DSP-based CD compensation filter. Assume that the fiber type is homogenous across the network (which is reasonable but of course not always true), the digital coherent receiver is able to provide a rough estimate of the link transmission distance. In any case, according to Fig. 7 and 9, it can be deduced that with a large distance estimation error up to 100 km, the corresponding  $\xi$  (obtained from look-up table) will deviate by at most 0.3 dB from the optimal value, which translates into another 0.2 dB OSNR estimation error for PM-QPSK systems and 0.4 dB for PM-16-QAM systems. Therefore, our technique is rather insensitive to inaccurate estimation of transmission distance.

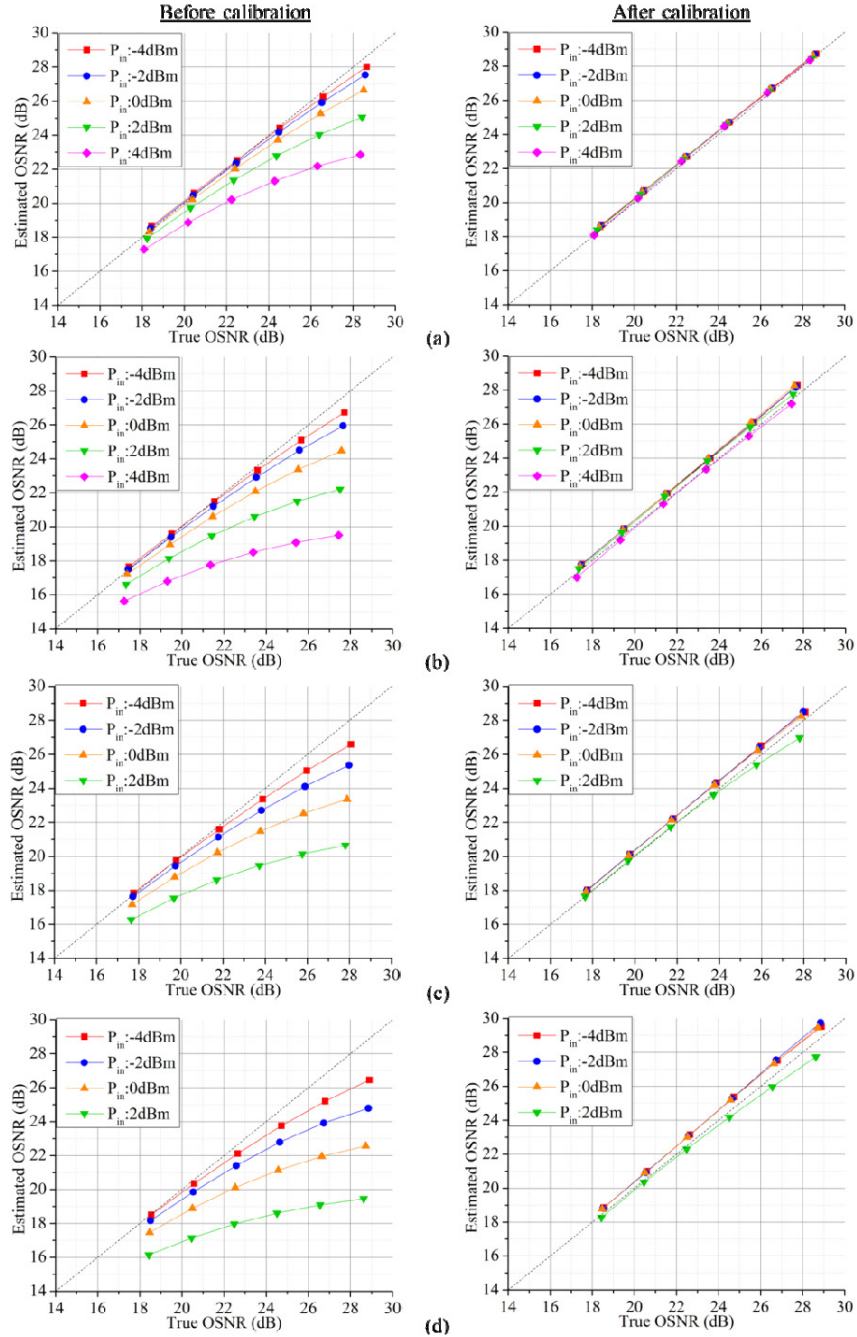


Fig. 8. Estimated OSNR vs true OSNR for a 224 Gb/s PM-16-QAM system obtained from simulations for various signal launched powers and OSNR values (a) after 400km transmission and calibrated with  $\xi = 11.2$ . The maximum estimation error is 0.9 dB; (b) after 800 km transmission and calibrated with  $\xi = 12.3$ . The maximum estimation error is 1.73 dB; (c) after 1200 km transmission calibrated with  $\xi = 12.8$ . The maximum estimation error is 1.81 dB; (d) after 1600 km transmission calibrated with  $\xi = 13.8$ . The maximum estimation error is 1.98 dB. Different pulse shapes, timing phases, PDL and DGD with different SOPs are considered in the simulation and estimation results.

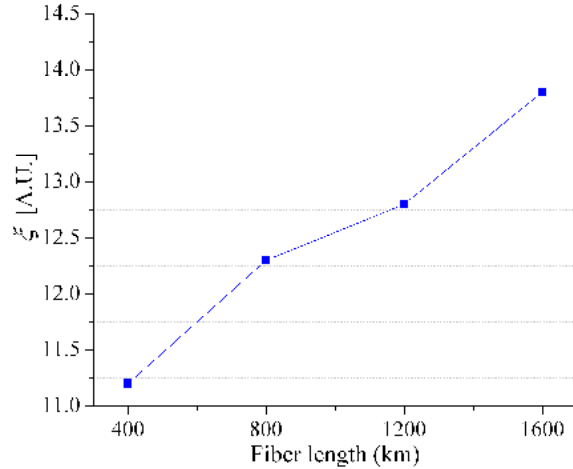


Fig. 9. The optimized calibration factor  $\xi$  vs. transmission distance for a 224 Gb/s PM-16-QAM system for realizing nonlinearity-insensitive OSNR monitoring.

In addition, we briefly investigated the performance of the proposed OSNR monitoring technique in WDM systems. In the presence of inter-channel nonlinear effects such as cross-phase modulation (XPM) and four-wave mixing (FWM), the signals are further degraded by the additional nonlinear distortions. However, those additional nonlinear distortions can be calibrated into our EVM-based OSNR estimator using a larger  $\xi$ . The optimized  $\xi$  versus transmission distance for a multi-channel 224 Gb/s PM-16-QAM system with 50 GHz channel spacing is shown in Fig. 10. We can see that with inter-channel nonlinear impairments the optimal  $\xi$  increases with the number of channels and saturates when the number of channels exceeds 9. This is in agreement with expectations as channels spaced far apart interact less with each other through XPM due to walk-off effects. For a 21-channel WDM system, the maximum monitoring errors are 0.8 dB, 1.1 dB, 1.5 dB and 2.2 dB for 400 km, 800 km, 1200 km and 1600 km transmissions respectively.

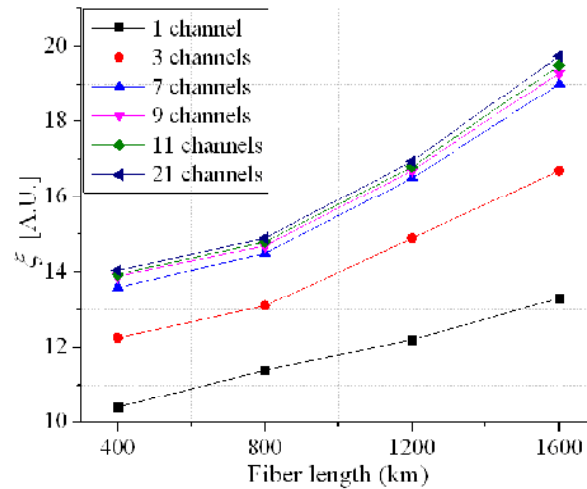


Fig. 10. The optimized calibration factor  $\xi$  vs. transmission distance for a 224 Gb/s PM-16-QAM WDM system for realizing nonlinearity-insensitive OSNR monitoring. The channel spacing is 50 GHz.

#### **4. Conclusions**

In this paper, we proposed a fiber-nonlinearity-insensitive OSNR monitoring technique for digital coherent receivers by incorporating and calibrating fiber nonlinearity-induced amplitude noise correlations among neighboring symbols into conventional OSNR estimation techniques from received signal distributions. For 112Gb/s PM-QPSK systems, accurate OSNR monitoring in the range of 10–24 dB is experimentally demonstrated by the proposed technique in presence of relatively strong fiber nonlinearity. For 224 Gb/s PM-16-QAM systems, simulation results demonstrated accurate OSNR monitoring in the range of 18-28 dB and the proposed OSNR monitoring technique is shown to be robust against different signal pulse shapes, timing phase offsets, PDL and first-order PMD effects. Finally, studies on multi-channel 224 Gb/s PM-16-QAM WDM systems demonstrated the validity of the proposed OSNR monitoring technique in the presence of inter-channel nonlinearities. Further investigations on the proposed methodology to potentially isolate ASE noise, SPM and XPM effects will be attempted in the future.

#### **Acknowledgments**

The authors would like to acknowledge the support of the Hong Kong Government General Research Fund under project number PolyU 519910.